Collective Modes in 2-D Yukawa Solids and Liquids

Péter Hartmann, Zoltán Donkó, Gabor J. Kalman, Stamatios Kyrkos,
Marlene Rosenberg, *Member, IEEE*, and Pradip M. Bakshi

Abstract—We report comparative studies on collective excitations in 2-D complex plasmas, in which particles interact through the Yukawa potential, encompassing both the solid and the strongly coupled liquid states. Dispersion and polarization of the collective modes in the solid state are calculated through the lattice summations, while in the liquid state, through molecular dynamics (MD) simulations in conjunction with the theoretical quasi-localized charge approximation analysis. The latter closely emulates the dispersion, resulting from an angular averaging in the lattice. In general, however, the lattice dispersion is substantially different from that of the liquid. The MD simulations show the dramatic transformation of the anisotropic phonon dispersion of the crystal lattice near the solid–liquid transition into the isotropic liquid dispersion.

Index Terms—Molecular dynamics (MD) simulation, phonon dispersion, strongly coupled plasma, 2-D Yukawa system.

I. Introduction

THE interparticle interaction between the dust particles in a single complex plasma layer can be modeled by the Yukawa potential $\Phi(r) = (Q^2/r)e^{-\kappa r}$, where Q is the charge of the particles. We further assume equal mass and charge for all particles. This model system can fully be parameterized by two dimensionless quantities: the Coulomb coupling parameter $\Gamma = \beta(Q^2/a)$ and the screening parameter $\bar{\kappa} = \kappa a$, where $\beta = 1/k_B T$, T is the temperature, $a = (\pi n)^{-1/2}$ is the 2-D Wigner–Seitz radius, and n is the particle number surface density. In the following, we use a as the length unit (e.g., $\bar{r} = r/a$, $\bar{k} = ka$) and $\omega_p = \sqrt{2\pi Q^2 n/ma}$ as the frequency unit, where m is the mass of the particles. For a perfect triangular lattice, the conversion between Wigner–Seitz (a) and lattice-length (b) units can be performed using the equality $b^2 = a^2 2\pi/\sqrt{3}$.

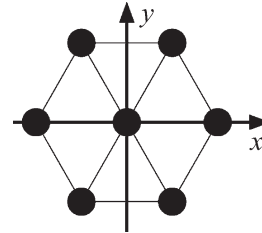In the following, we briefly introduce the three methods applied in our studies.

Fig. 1. Schematic orientation of the triangular lattice.

A. Lattice Calculations

Lattice summation technique is used to study the system in the zero-temperature limit (ground state). This method is based on the harmonic approximation where the particles oscillate around their equilibrium positions in a local potential well, created by all other particles. The amplitude of the oscillation is infinitesimal; therefore, the shape of the potential well can be approximated with a quadratic surface, and anharmonic effects can be neglected [1], [2].

The dispersion relations of plane waves can be obtained by solving the eigenvalue problem [1]

$$\left\| \omega^2(k,\varphi)\delta_{\mu\nu} - D_{\mu\nu}(\mathbf{k}) \right\| = 0 \qquad (1)$$

where $\mathbf{k}$ is the wavenumber vector and φ is the propagation angle (with respect to a predefined direction, the x-axis in this case, pointing toward the nearest neighbor, see Fig. 1). $D_{\mu\nu}(\mathbf{k})$ is the dynamical matrix defined as

$$D_{\mu\nu}(\mathbf{k}) = -\frac{1}{m}\sum_i \frac{\partial^2\Phi(r_i)}{\partial r_{i\mu}\partial r_{i\nu}}(e^{i\mathbf{k}\cdot\mathbf{r}_i} - 1) \qquad (2)$$

where $\mathbf{r}_i$ is the position and $\Phi(r_i)$ is the potential contribution of the ith triangular lattice site, respectively. Summation runs over all lattice sites with $0 < r_i < R$, where R is the cutoff radius (which is, e.g., of the order of 40 lattice side lengths for a $\bar{\kappa} = 2$ system).

B. Molecular Dynamics (MD) Simulation

The numerical simulation is based on the MD method [3] using a rectangular simulation box and periodic boundary conditions. The exponential decay of the Yukawa interaction potential makes it possible to introduce a cutoff radius R_{cut}. Only the particle pairs separated by less than R_{cut} are taken into account in the force calculation in the solution of Newton's equation of motion. R_{cut} is determined by the screening parameter κ and is defined to produce a relative error $< 10^{-9}$ in the force calculation. In the present case (for $\bar{\kappa} = 2$), $R_{\text{cut}} \approx$

$12a \approx 0.1L$, where L is the simulation box side length. At the beginning of the simulations, the $N = 3960$ particles are situated at the triangular lattice sites (oriented as shown in Fig. 1), with random velocities sampled from a Maxwellian distribution. Following an initialization period, during which the velocities of the particles are scaled back in each time step to maintain the prescribed value of the temperature, the system reaches its stationary state and the particles move without any thermostation. Our computer experiments are performed in this second "measurement" phase of the simulation, where the total energy is conserved (with a relative error of $< 10^{-6}$) and the instantaneous temperature (calculated from the per particle average kinetic energy using $\langle (1/2)mv^2 \rangle = k_B T$) fluctuates around its equilibrium value.

Longitudinal and transverse current fluctuation spectra are obtained through the Fourier transforms [4]

$$L(k, \omega) = \frac{1}{2\pi N} \lim_{\Delta t \to \infty} \frac{1}{\Delta t} |\mathcal{F}\{\lambda(k, t)\}|^2$$

$$T(k, \omega) = \frac{1}{2\pi N} \lim_{\Delta t \to \infty} \frac{1}{\Delta t} |\mathcal{F}\{\tau(k, t)\}|^2 \tag{3}$$

of the microscopic quantities

$$\lambda(k, t) = k \sum_j v_{jx} \exp(ikx_j)$$

$$\tau(k, t) = k \sum_j v_{jy} \exp(ikx_j) \tag{4}$$

where the index j runs over all particles and Δt in (3) is the duration of data recording. In the MD simulations, only two directions of propagation are considered: along the x- and y-axes [for the latter, x and y are interchanged in (4)]. Dispersion curves represent the spectral peak positions.

C. Quasi-Localized Charge Approximation (QLCA) Calculations

The concept of the QLCA theory is based on the separability of particle-oscillation and diffusion time scales in the strongly coupled liquid phase [5], [6]. The validity of this assumption for the strongly coupled liquids has already been proven in earlier studies [7]. The liquid phase can be described in terms of the isotropic equilibrium pair correlation function $g(r)$. To obtain the phonon dispersion, one then has to solve the eigenvalue problem

$$\left\| \omega^2(k, \varphi)\delta_{\mu\nu} - \Omega_0^2(k)\frac{k_\mu k_\nu}{k^2} - D_{\mu\nu}(\mathbf{k}) \right\| = 0 \tag{5}$$

where now

$$D_{\mu\nu}(\mathbf{k}) = -\frac{n}{m}\int \frac{\partial^2 \Phi(r)}{\partial r_{i\mu}\partial r_{i\nu}} (e^{i\mathbf{k}\cdot\mathbf{r}_i} - 1)[g(r) - 1]\,dr. \tag{6}$$

The $g(r)$ is the pair-correlation function, which is obtained from our MD simulations. Ω_0 is the Vlasov value of the
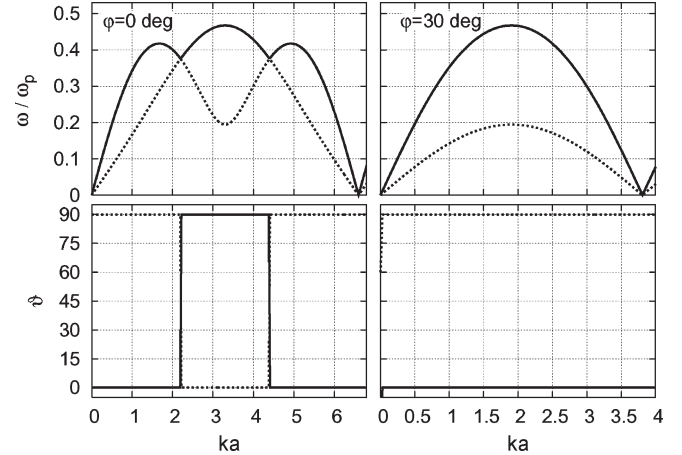

Fig. 2. Lattice normal mode dispersions and polarization angles (ϑ) for the two principal directions $\varphi = 0°$ and $30°$. The polarization is the angle between the normal mode eigenvectors and the wavenumber vector $\mathbf{k}$. Full and dotted lines represent the data of the two eigenmodes for $\bar{\kappa} = 2$.

longitudinal plasmon frequency for a 2-D Yukawa system

$$\frac{\Omega_0^2(\bar{k})}{\omega_p^2} = \frac{\bar{k}^2}{\sqrt{\bar{k}^2 + \bar{\kappa}^2}}. \tag{7}$$

The above equations result in the following dispersion formulas for the longitudinal and transverse modes:

$$\omega_L^2/\omega_p^2 = \frac{\bar{k}^2}{2}\int_0^\infty \Lambda(kr, \kappa r)g(r)d\bar{r}$$

$$\omega_T^2/\omega_p^2 = \frac{\bar{k}^2}{2}\int_0^\infty \Theta(kr, \kappa r)g(r)d\bar{r} \tag{8}$$

with

$$\Lambda(x, y) = \frac{e^{-y}}{x^2}\left[(1 + y + y^2) - (4 + 4y + 2y^2)J_0(x)\right.$$
$$\left. + (6 + 6y + 2y^2)\frac{J_1(x)}{x}\right]$$

$$\Theta(x, y) = 2\frac{e^{-y}}{x^2}(1 + y + y^2)[1 - J_0(x)] - \Lambda(x, y) \tag{9}$$

where $J_0(x)$ and $J_1(x)$ are the Bessel functions of the first kind.

II. COMPARISON OF THE RESULTS

In this section, we compare the results obtained using the methods discussed in Section I, both with each other and with the experimental results of Piel *et al.* [8].

1) Lattice Dispersion: While it is sufficient to consider $\mathbf{k}$ values within the first Brillouin zone to obtain a full information on the frequency spectrum, it is instructive to follow the dispersion for high values of k and study the angular dependence of the periodicity of the $\omega(\mathbf{k})$ curves. Simple periodicity of $\omega(\mathbf{k})$ in k prevails only in the principal directions of the lattice (Fig. 2). In a general direction $0 \leq \varphi \leq 30°$, the period in k is
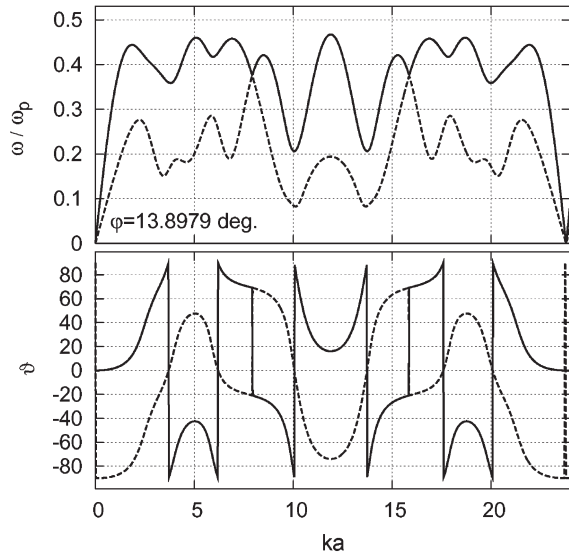
Fig. 3. Lattice normal mode dispersions and polarization angles (ϑ) for a direction corresponding to $m = 4$ and $n = 10$ ($\varphi = 13.8979°$). The periodicity in this case is $\bar{k} = ka = 23.7891$. $\bar{\kappa} = 2$.

given by [9]

$$\tilde{k}_{\text{period}} = \frac{4\pi}{\sqrt{3}}\sqrt{m^2 + mn + n^2} \tag{10}$$

in the lattice-length units, where m and n are minimal integers satisfying

$$\tan\left(\frac{\pi}{6} - \varphi\right) = \frac{m\sqrt{3}}{m + 2n}. \tag{11}$$

Moreover, "longitudinal" and "transverse" polarizations occur only in the principal directions, while in general, the polarizations are mixed and the polarization angle ϑ (the angle between the normal mode eigenvectors and the wavenumber vector $\mathbf{k}$) is a sensitive function of k and φ (Fig. 3).

Longitudinal (L) and transverse (T) modes can be projected based on the normal-mode data with

$$\omega_L^2 = (\hat{\mathbf{k}} \cdot \hat{\mathbf{e}}_1)^2 \omega_1^2 + (\hat{\mathbf{k}} \cdot \hat{\mathbf{e}}_2)^2 \omega_2^2$$
$$\omega_T^2 = \left[1 - (\hat{\mathbf{k}} \cdot \hat{\mathbf{e}}_1)^2\right]\omega_1^2 + \left[1 - (\hat{\mathbf{k}} \cdot \hat{\mathbf{e}}_2)^2\right]\omega_2^2 \tag{12}$$

where $\hat{\mathbf{k}}$, $\hat{\mathbf{e}}_1$, and $\hat{\mathbf{e}}_2$ are the unit vectors parallel to the wavenumber ($\mathbf{k}$) and normal-mode eigenvectors ($\mathbf{e}_1$ and $\mathbf{e}_2$), respectively. ω_1 and ω_2 are the normal-mode frequencies.

2) Lattice Versus MD: Lattice dispersions represent the $T = 0$ ground state situation. Finite temperature dispersions in the solid phase can be computed with the MD simulation method. For comparison with the lattice data, we have performed a simulation at a very low temperature with a coupling parameter $\Gamma = 10^4$ and with particles initially placed at the lattice sites. In the simulations, the measurements are performed along the two principal directions ($\mathbf{k}$ parallel to x- and y-axes). Due to the hexagonal symmetry of the underlying lattice, the $\varphi = 90°$ and $\varphi = 30°$ cases are equivalent.

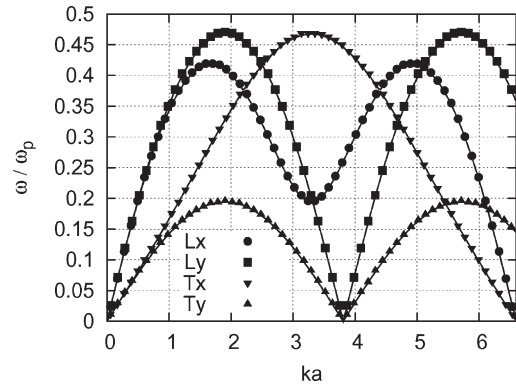The comparison in Fig. 4 shows a very close agreement between the two methods. Since the lattice calculations rests

Fig. 4. Lattice (lines) and MD dispersions (symbols) for $\Gamma = 10^4$ and $\bar{\kappa} = 2$. Compared are both x ($0°$, L_x/T_x) and y ($90°$, L_y/T_y lattice equivalent is $\varphi = 30°$) $\mathbf{k}$ directions.
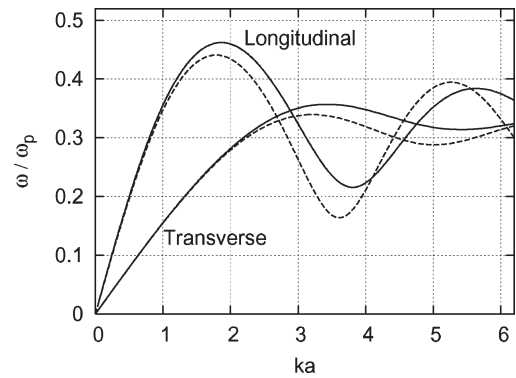

Fig. 5. Angularly averaged lattice (dashed lines) and QLCA (solid lines) dispersions of longitudinal and transverse modes using pair-correlation ($g(r)$) data from an MD simulation at $\Gamma = 360$ and $\bar{\kappa} = 2$.

on solid foundations, this agreement verifies the consistency of the computational procedure.

3) Lattice Average Versus QLCA: The QLCA describes the collective behavior of the strongly coupled isotropic liquids, and therefore, a direct comparison of the QLCA results with those of the lattice calculations cannot be done. Nevertheless, on the microscopic level, the strongly coupled liquid systems still emulate an anisotropic lattice environment (with random orientation of the principal axes), and thus, comparison of the QLCA results with an *angularly averaged* longitudinal (L) and transverse (T) lattice mode dispersions, in fact, is useful. This comparison is shown in Fig. 5.

4) Solid–Liquid Transition: The changes in the dynamical properties of the system during the solid–liquid phase transition can be monitored by performing a series of MD simulations in the vicinity of the expected phase transition temperature ($\Gamma_m \approx 415$ for $\bar{\kappa} = 2$) [10]. Fig. 6 shows L and T dispersions in both principal directions for three different values of the coupling.

$\Gamma = 500$ represents a relatively high-temperature solid, where lattice defects may already show up, but the overall behavior (sharp separation of the x- and y-directions) reflects the conservation of the triangular crystalline structure.

The $\Gamma = 405$ case corresponds to a temperature slightly higher than the melting temperature, where all long-range order in the system has already been extinguished, but locally, most of the particles sit in the somewhat distorted hexagonal
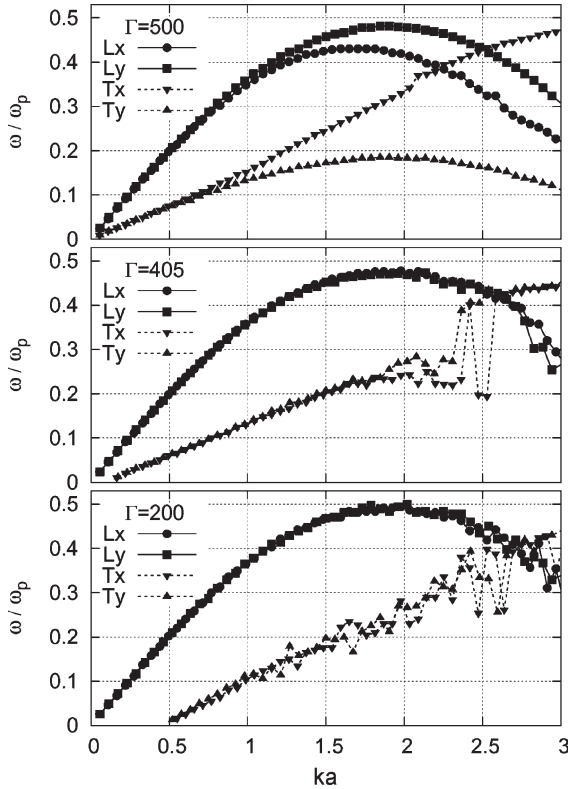
Fig. 6. Comparison of MD (L and T) dispersions in the solid phase ($\Gamma = 500$), just after melting ($\Gamma = 405$) and in the liquid phase ($\Gamma = 200$) for $\bar{\kappa} = 2$. Shown are both x and y polarizations.

environment. The "oscillatory" feature in the T mode around $ka = 2.5$ can be taken as an indication for the transition from the ordered lattice to the disordered liquid state through the formation of disoriented domains of the local hexagonal order. The orientations of these domains become more decorrelated with increasing temperature.

The $\Gamma = 200$ system is a typical strongly coupled liquid. Most prominent features are the isotropy of the dispersion (x- and y-directions are equivalent) and the appearance of a finite wavenumber cutoff for the T mode. This can be explained by the fact that liquids are not able to sustain long-wavelength shear modes.

5) MD Liquid Versus QLCA: In the liquid phase, both the MD and QLCA methods are applicable. In fact, the QLCA uses the pair-correlation functions (e.g., from MD simulations) as the input data. Getting the $g(r)$ from the MD simulation is, however, computationally much cheaper than computing the dynamical fluctuation spectra and dispersions. Besides its analytic nature, this computational efficiency is the main advantage of the QLCA method.

To test the accuracy of the different approaches, we have performed the MD simulations for a series of Γ and κ parameters. Fig. 7 shows, as an example, the dispersion curves of the longitudinal mode for $\Gamma = 120$ and $\bar{\kappa} = 0, 1, 2,$ and 3 [11], [12].

6) QLCA Versus Experiment: For a theoretical work it is essential to obtain a link to the experimental findings. The comparison of transverse mode dispersions with the experiments in the liquid phase is made possible by using the results of
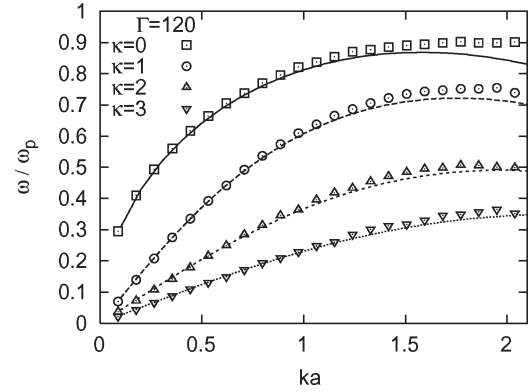

Fig. 7. Comparison of MD (symbols) and QLCA (lines) longitudinal dispersion relations for $\Gamma = 120$ and $\bar{\kappa} = 0, 1, 2,$ and 3.
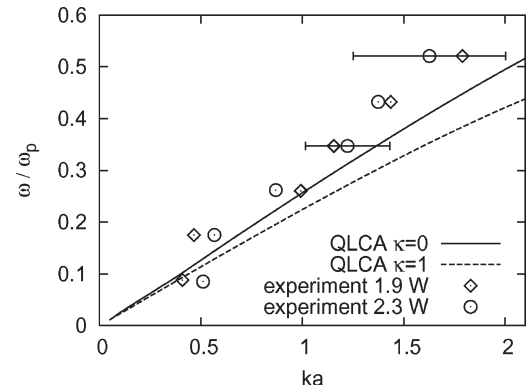

Fig. 8. Comparison of QLCA (lines) transverse dispersions for $\bar{\kappa} = 0$ and 1 with experimental results for 1.9- and 2.3-W laser heating powers taken from [8].

Piel, Nosenko, and Goree, as shown in Fig. 8. The experiment was carried out in a modified GEC reference cell. Spherical dust particles were injected into a room-temperature argon gas discharge powered at 13.56 MHz. The temperature of the levitating particle suspension was controlled using external laser beams at powers of 1.9 and 2.3 W. Shear waves were excited by an additional laser beam and were identified by recording particle coordinates, followed by spatial Fourier analysis (for more details, see [8]).

Since the comparison is made in absolute quantities, the overall agreement between the experiment and the 2-D QLCA model is quite satisfying.

III. SUMMARY

We have investigated the 2-D Yukawa systems in the solid and liquid phases through various theoretical and computational approaches. Lattice calculations provide a reliable reference data for the system in the ground state. MD simulations are capable of investigating the system in the full strongly coupled domain, based on very few approximations (first principles). The QLCA is a semianalytic approach useful for theoretical investigations in the isotropic (liquid) phase. Comparative studies (using all of these methods) provide valuable information about the reliability of the methods and the accuracy of the results.

ACKNOWLEDGMENT

REFERENCES

[1] L. Bonsall and A. A. Maradudin, "Some static and dynamical properties of a two-dimensional Wigner crystal," *Phys. Rev. B, Condens. Matter*, vol. 15, no. 4, pp. 1959–1973, Feb. 1977.

[2] H. E. De Witt, W. L. Slattery, A. I. Chungunov, D. A. Baiko, and D. G. Yakovlev, "Pair distribution of ions in Coulomb lattice," *J. Phys., A, Math. Gen.*, vol. 36, no. 22, pp. 6221–6226, Jun. 2003.

[3] D. Frenkel and B. Smit, *Understanding Molecular Simulation*. New York: Academic, 1996.

[4] J. P. Hansen, I. R. McDonald, and E. L. Pollock, "Statistical mechanics of dense ionized matter. III. Dynamical properties of the classical one-component plasma," *Phys. Rev. A, Gen. Phys.*, vol. 11, no. 3, pp. 1025–1039, Mar. 1975.

[5] K. I. Golden and G. J. Kalman, "Quasilocalized charge approximation in strongly coupled plasma physics," *Phys. Plasmas*, vol. 7, no. 1, pp. 14–32, Jan. 2000.

[6] G. J. Kalman, K. I. Golden, Z. Donkó, and P. Hartmann, "The quasilocalized charge approximation," *J. Phys. Conf. Series*, vol. 11, pp. 254–267, 2005.

[7] Z. Donkó, G. J. Kalman, and K. I. Golden, "Caging of particles in one-component plasmas," *Phys. Rev. Lett.*, vol. 88, no. 22, p. 225 001, May 2002.

[8] A. Piel, V. Nosenko, and J. Goree, "Laser-excited shear waves in solid and liquid two-dimensional dusty plasmas," *Phys. Plasmas*, vol. 13, no. 4, p. 042 104, Apr. 2006.

[9] T. Sullivan, G. J. Kalman, S. Kyrkos, P. Bakshi, M. Rosenberg, and Z. Donkó, "Phonons in Yukawa lattices and liquids," *J. Phys., A, Math. Gen.*, vol. 39, no. 17, pp. 4607–4611, Apr. 2006.

[10] P. Hartmann, Z. Donkó, P. Bakshi, G. J. Kalman, and S. Kyrkos, "Molecular dynamics studies of the solid–liquid phase transition in 2-D Yukawa Systems," *IEEE Trans. Plasma Sci.*, vol. 35, no. 2, pp. 332–336, Apr. 2007.

[11] G. J. Kalman, P. Hartmann, Z. Donkó, and M. Rosenberg, "Two-dimensional Yukawa liquids: Correlation and dynamics," *Phys. Rev. Lett.*, vol. 92, no. 6, p. 065 001, Feb. 2004.

[12] P. Hartmann, Z. Donkó, K. Kutasi, and G. J. Kalman, "Equilibrium properties and phase diagram of two-dimensional Yukawa systems," *Phys. Rev. E, Stat. Phys. Plasmas Fluids Relat. Interdiscip. Top.*, vol. 72, no. 8, p. 026 409, Aug. 2005.

Zoltán Donkó was born in Ózd, Hungary, in 1965. He received the degree and the Doctoral degree from Technical University of Budapest, in 1989 and 1992, respectively. He also received the C.Sc. and D.Sc. degrees from the Hungarian Academy of Sciences in 1996 and 2006, respectively.

Currently, he is the Head of the Department of Laser Physics, Research Institute for Solid State Physics and Optics of the Hungarian Academy of Sciences. His research interest includes the physics of strongly coupled plasmas and of low-pressure gas discharges.

Gabor J. Kalman received the D.Sc. degree from the Israel Institute of Technology, Haifa, Israel, in 1962.

He is a Distinguished Research Professor at the Department of Physics, Boston College, Chestnut Hill, MA. His research interests include strongly coupled Coulomb systems, linear and nonlinear response functions, and fluctuation-dissipation theorems.

Dr. Kalman is a Fellow of the American Physical Society and the New York Academy of Sciences.

Stamatios Kyrkos received the Ph.D. degree from Boston College, Chestnut Hill, MA, in 2003.

He is an Assistant Professor of physics with the Department of Chemistry and Physics, Le Moyne College, Syracuse, NY. His research interests include linear and nonlinear response functions, compressibilities, screening, strongly coupled Coulomb systems (plasmas, 2-D, and 3-D electron liquid), and charged particle bilayers.

Marlene Rosenberg (M'88) received the B.A. degree from University of Pennsylvania, Philadelphia, and the M.A. and Ph.D. degrees in astronomy from Harvard University, Cambridge, MA.

After a Postdoctoral Position at Oxford University, Oxford, U.K., she was a Senior Scientist with the General Atomics and then with the Jaycor, San Diego, CA. She is currently a Research Scientist with the Department of Electrical and Computer Engineering, University of California, San Diego. Her current research interests include the physics of dusty plasmas. Her research interests have included theoretical plasma physics applied to nuclear fusion and related subjects.

Dr. Rosenberg is a member of the American Physical Society (APS), American Geophysical Union (AGU), and International Union of Radio Science (URSI).

Péter Hartmann received the Ph.D. degree in physics from Eötvös Loránd University, Budapest, Hungary, in 2004.

He is a Postdoctoral Research Fellow with the Research Institute for Solid State Physics and Optics of the Hungarian Academy of Sciences. His research interests include experimental and simulational investigations of elementary processes in low-pressure gas discharges and numerical studies of strongly coupled plasmas.

Pradip M. Bakshi received the Ph.D. degree from Harvard University, Cambridge, MA, in 1962.

He is a Distinguished Research Professor with the Department of Physics, Boston College, Chestnut Hill, MA. His research interests include quantum field theory, plasma physics, and condensed matter physics.